Article

pubs.acs.org/Biomac

Bioimaging of Hyaluronic Acid Derivatives Using Nanosized Carbon Dots

Eun Ji Goh,[†,∥] Ki Su Kim,[†,∥] Yi Rang Kim,[‡] Ho Sang Jung,[†] Songeun Beack,[†] Won Ho Kong,[†] Giuliano Scarcelli,[§] Seok Hyun Yun,[‡,§] and Sei Kwang Hahn*[,†,§]

[†]Department of Materials Science and Engineering, Pohang University of Science and Technology (POSTECH), San 31, Hyoja-dong, Nam-gu, Pohang, Kyungbuk, 790-784, Korea

[‡]Graduate School of Nanoscience and Technology (WCU), Korea Advanced Institute of Science and Technology (KAIST), 335 Gwahak-ro, Yusong-gu, Daejon, 305-701, Korea

[§]Wellman Center for Photomedicine, Harvard Medical School and Massachusetts General Hospital, 65 Landsdowne Street UP-5, Cambridge, Massachusetts 02139, United States

ABSTRACT: Fluorescent nanosized carbon dots (Cdots) are an emerging bioimaging agent with excellent chemical inertness and marginal cytotoxicity in comparison to widely used semiconductor quantum dots. In this work, we report the application of Cdots for real time bioimaging of target specific delivery of hyaluronic acid (HA) derivatives. Polyethylene glycol (PEG) diamine-capped Cdots were synthesized by the pyrolysis of citric acid in a hot solvent. The synthesized Cdots showed strong fluorescence under UV excitation with emission properties dependending on the excitation wavelength. HA−Cdot conjugates were synthesized by amide bond formation between amine groups of Cdot and carboxylic groups of HA. After confirmation of the negligible cytotoxicity of Cdots and HA−Cdot conjugates, in vitro bioimaging was carried out for target specific intracellular delivery of the HA−Cdot conjugates by HA receptor-mediated endocytosis. Furthermore, in vivo real-time bioimaging of Cdots and HA−Cdot conjugates exhibited the target specific delivery of HA−Cdot conjugates to the liver with abundant HA receptors. Taken together, we could confirm the feasibility of HA derivatives as a target-specific drug delivery carrier for the treatment of liver diseases and Cdots as a promising bioimaging agent.

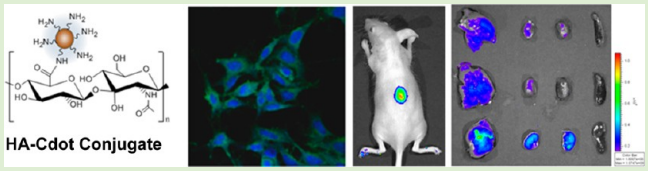

INTRODUCTION

A variety of nanomaterials, such as semiconductor quantum dots (Qdots), gold nanoparticles, superparamagnetic iron oxides, and carbon materials, have been extensively investigated for various bioimaging applications.[1−4] These nanosized contrast agents have made it possible to observe specific biological events noninvasively with advantages over the conventional organic fluorescent dyes in terms of stability, resistance to photobleaching, metabolic disintegration, and adequate dispersibility in a biological environment.[5] Among the bioimaging agents, semiconductor Qdots have been exploited to label biomolecules with a wide range of colors on the basis of size-tunable photoluminescence (PL)[3] and a high quantum yield.[6−8] However, the major concern for Qdots is their cytotoxicity due to the use of cadmium and other heavy metal constituents.[9] To alleviate this problem, the surface of Qdots were modified with silica, cytocompatible phospholipids, polyethylene glycol (PEG), and so on.[10−12] In addition, the particle size of Qdots was made below 5 nm to facilitate the rapid renal clearance,[13] and biofriendly QDots were synthesized using cytocompatible metals such as Mn-doped ZnS.[14,15] Despite these efforts, the inherent cytotoxicity of Qdots is one of the major obstacles for their further clinical applications.

Meanwhile, carbon materials such as graphene oxides (GOs) and single-walled carbon nanotubes (SWNTs) have been investigated for bioimaging applications.[16−19] Nanosized GO showed strong visible, ultraviolet, or near-infrared (NIR) fluorescence by the recombination of electron−hole pairs in localized electron states made of heterogeneous atomic and electronic structures.[20] SWNTs also showed remarkably stable fluorescence at the NIR region.[21] GOs and SWNTs have been exploited for in vitro and in vivo bioimaging drawing many attentions as potential biocompatible imaging agents.[22−25] Recently, fluorescent nanosized carbon dots (Cdots) have been also suggested for bioimaging applications.[25,26] Cdots were found first in the purification process of SWNTs.[25] Since then, many approaches have been performed to synthesize Cdots from top-down methods, such as arc-discharge, laser-ablation method, and electrochemical oxidation, to bottom-up methods, such as combustion, thermal decomposition, and microwave synthesis.[26−28] Cdots have many advantages, such as chemical inertness, lack of blinking, inherently low cytotoxicity, excellent biocompatibility, size- and excitation-wavelength (λ_{ex})-dependent PL, and amphiphilic characteristics depending on the surface capping materials.[26,30−33]

In this work, we carried out real-time bioimaging for the target specific delivery of hyaluronic acid (HA) derivatives

Received: May 21, 2012
Revised: July 13, 2012
Published: July 17, 2012

Scheme 1. Schematic Illustration for the Synthesis of (a) Cdots Using Citric Acid and PEG-Diamine, and (b) HA−Cdot Conjugates Using the EDC Chemistry

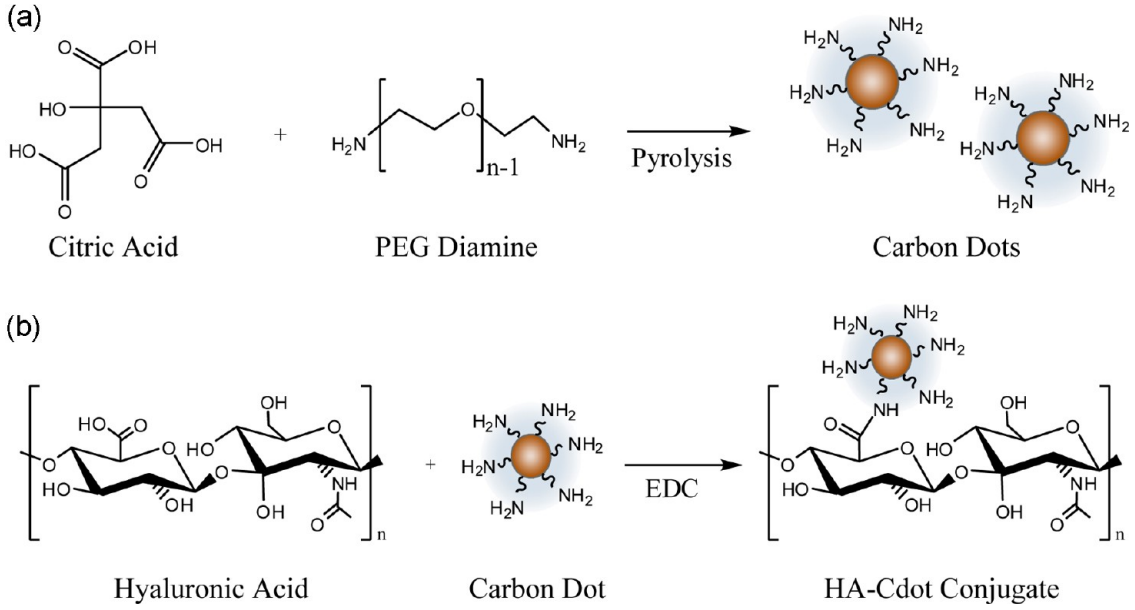

using Cdots. HA is a naturally occurring liner polysaccharide in the body, which is biodegradable, cytocompatible, nontoxic, and nonimmunogenic. HA has been investigated for target specific drug delivery applications by the HA receptor-mediated endocytosis.[34,35] Cluster determinant 44 (CD44), lymphatic vessel endothelial hyaluronan receptor (LYVE)-1, and HA receptor for endocytosis (HARE) have been identified as HA receptors for various biological functions in the body. After synthesis and characterization of PEG diamine-capped Cdots and HA−Cdot conjugates, in vitro and in vivo bioimaging were carried out for target specific delivery of HA derivatives. The results were discussed for further applications of HA derivatives as target specific drug delivery carriers for the treatment of liver diseases and Cdot as a promising bioimaging agent.

EXPERIMENTAL SECTION

Materials. Citric acid anhydrate was purchased from Alfa Aesar GmbH (Karlsruhe, Germany) and PEG diamine with a molecular weight (MW) of 2000 was obtained from Sunbio (Orinda, CA). Glycerin was purchased from Sigma-Aldrich (St. Louis, MO). Sodium salt of HA with an MW of 100 kDa was obtained from Shiseido (Tokyo, Japan) and 1-ethyl-3-(3-dimethyl-aminopropyl)carbodiimide hydrochloride (EDC) was purchased from Tokyo Chemical Industry (Tokyo, Japan). Dulbecco's modified Eagle medium (DMEM) and fetal bovine serum (FBS) were obtained from HyClone (Logan, UT), and 4′,6-diamidino-2-phenylindole (DAPI) was obtained from Molecular Probes (Carlsbad, CA). Double distilled water was used for the following experiments. All chemicals were used without further purification.

Synthesis and Characterization of Cdots. Cdots were synthesized as described elsewhere.[36] In brief, 9 mL of glycerin and 600 mg of PEG diamine were put into a 100 mL three-neck flask, which was degassed with nitrogen for 10 min. As the temperature increased to 270 °C, 600 mg of citric acid was quickly added into the flask, reacted at the temperature for 3 h, and then cooled down to room temperature. The resulting product was dialyzed against water using a cellulose ester dialysis membrane bag (molecular weight cutoff (MWCO) = 3500) to remove excess PEG diamine and glycerin. Ultraviolet/visible (UV/vis) spectra and PL spectroscopy were performed to measure the amount of Cdots with a changeable UV transilluminator (DUT-260, Core Bio System, Korea) and a

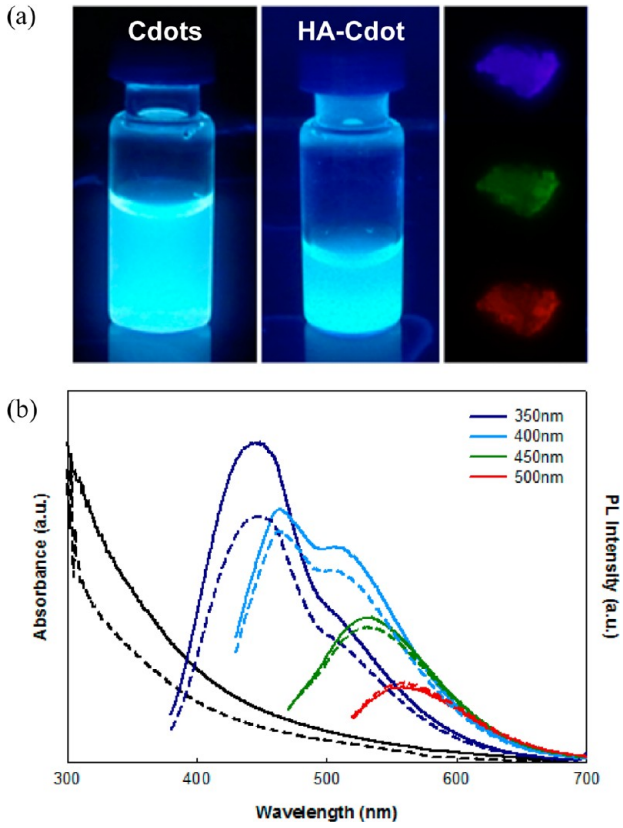

Figure 1. (a) Fluorescence images of Cdots (left) and HA−Cdot conjugates (middle) under UV light. Cdots exhibited a strong fluorescence under UV excitation and different fluorescence colors depending on the excitation wavelength (right). (b) UV/vis absorption and PL emission spectra of Cdots (solid lines) and HA−Cdot conjugates (dashed lines).

fluorescence spectrometer (FP-6500, JASCO, Japan). The morphology and size of Cdots were analyzed by atomic force microscopy (AFM, VEECO Instrument, New York, NY) and high-resolution transmission electron microscopy (HRTEM, JEOL 2100F, Tokyo) at

dx.doi.org/10.1021/bm300796q | Biomacromolecules 2012, 13, 2554−2561

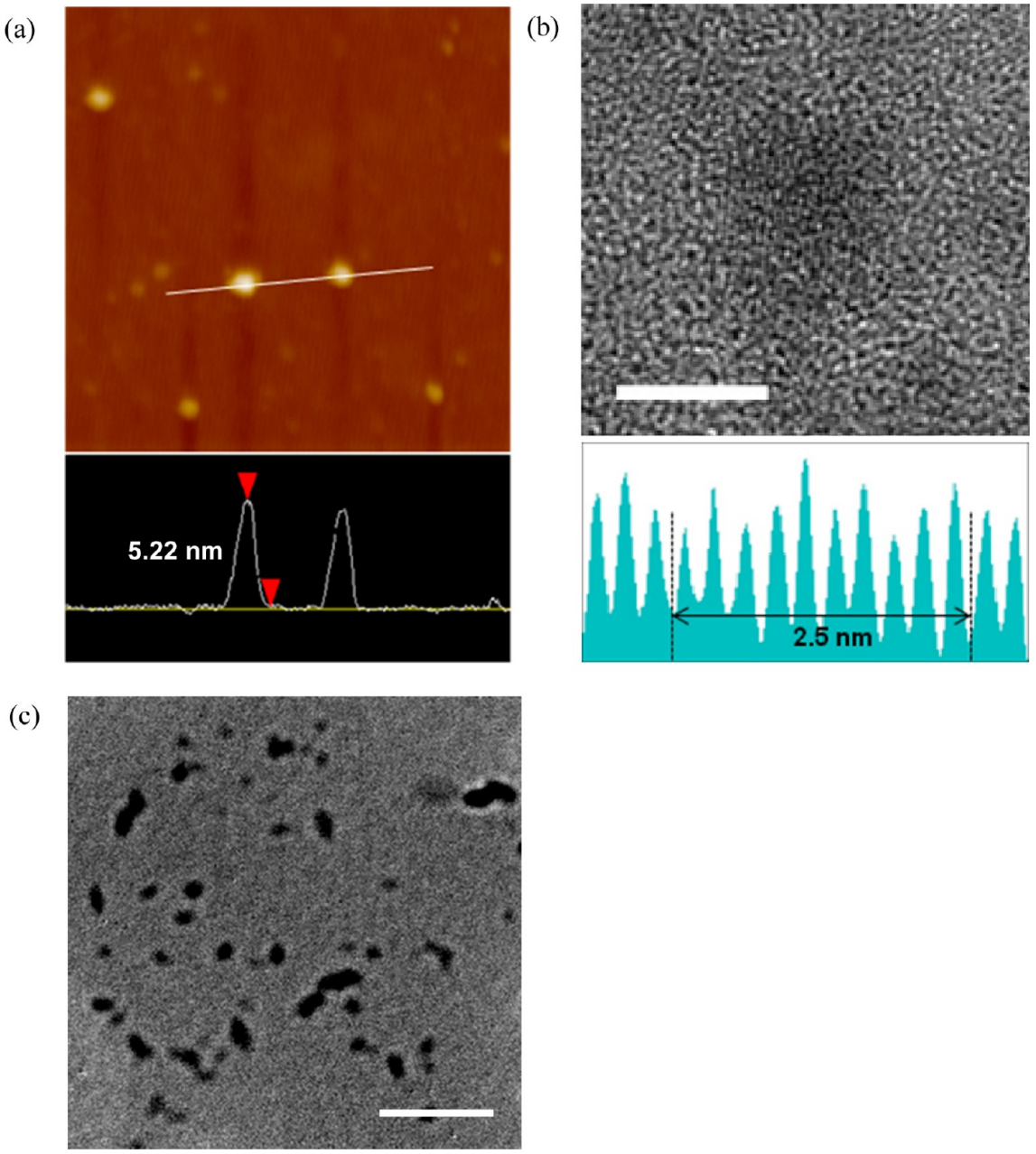

Figure 2. (a) AFM topographic image of Cdots with the height analysis. (b) HRTEM image of Cdots with the intensity profile (scale bar: 5 nm). (c) TEM image of HA−Cdot conjugates (scale bar: 250 nm).

an operating voltage of 200 kV. For the AFM analysis, each 100 μL of the Cdot and HA−Cdot conjugate solution was placed on a silicon wafer. The silicon wafer was air-dried overnight, and the remaining solution was blown away using an air-gun. The HRTEM specimens were prepared by drop-casting of 10 μL of Cdot solution on 300 mesh copper TEM grid with a carbon film followed by drying at room temperature.

Synthesis and Characterization of HA−Cdot Conjugates. HA was dissolved in water at a concentration of 5 mg/mL and mixed with 4-fold weight excess of Cdots. After adjusting the pH to 4.8 by the addition of 0.1 N HCl, the solution was mixed with 20-fold molar excess of EDC. During the reaction for the synthesis of HA-Cdot conjugate, the pH of the solution was consistently maintained at 4.8 for 2 h. Then, the pH of the solution was raised to 7.0 to terminate the reaction. The resulting solution was dialyzed and purified with a PD10 column. HA−Cdot conjugates were obtained by freeze-drying and stored in a refrigerator before use. The successful synthesis of HA-Cdot conjugate was assessed by TEM (Hitachi, Tokyo, Japan), ^{1}H nuclear magnetic resonance (NMR, DRX400, Bruker, Germany), and Fourier transform infrared spectroscopy (FT-IR, Nicolet 6700 FT-IR spectrometer, Thermo Fisher Scientific Co., Waltham, MA). The mean particle size of HA−Cdot conjugates was determined by measuring the sizes of 30 particles on the TEM images.

Cytotoxicity Tests of Cdots and HA−Cdot Conjugates. The cytotoxicity of Cdots and HA−Cdot conjugates was evaluated by MTS assay. Briefly, B16F1 and HEK293 cells were seeded on each well of 96 well-plate at a density of 8×10^3 cells/well, and cultured in a humidified 5% CO_2 incubator at 37 °C for 24 h. DMEM was supplemented with 10 vol% of FBS and 1 wt % of antibiotics. Fresh medium containing Cdots or HA−Cdot conjugates with increasing Cdot concentrations was added to each well and incubated for 24 h. Then, 20 μL of 0.2 mg/mL MTS solution in DMEM was added to each well and incubated at 37 °C for 2 h. Finally, the optical density was measured at 490 nm with an absorbance microplate reader (EMax microplate reader, Bucher Biotec AG, Basel, Switzerland).

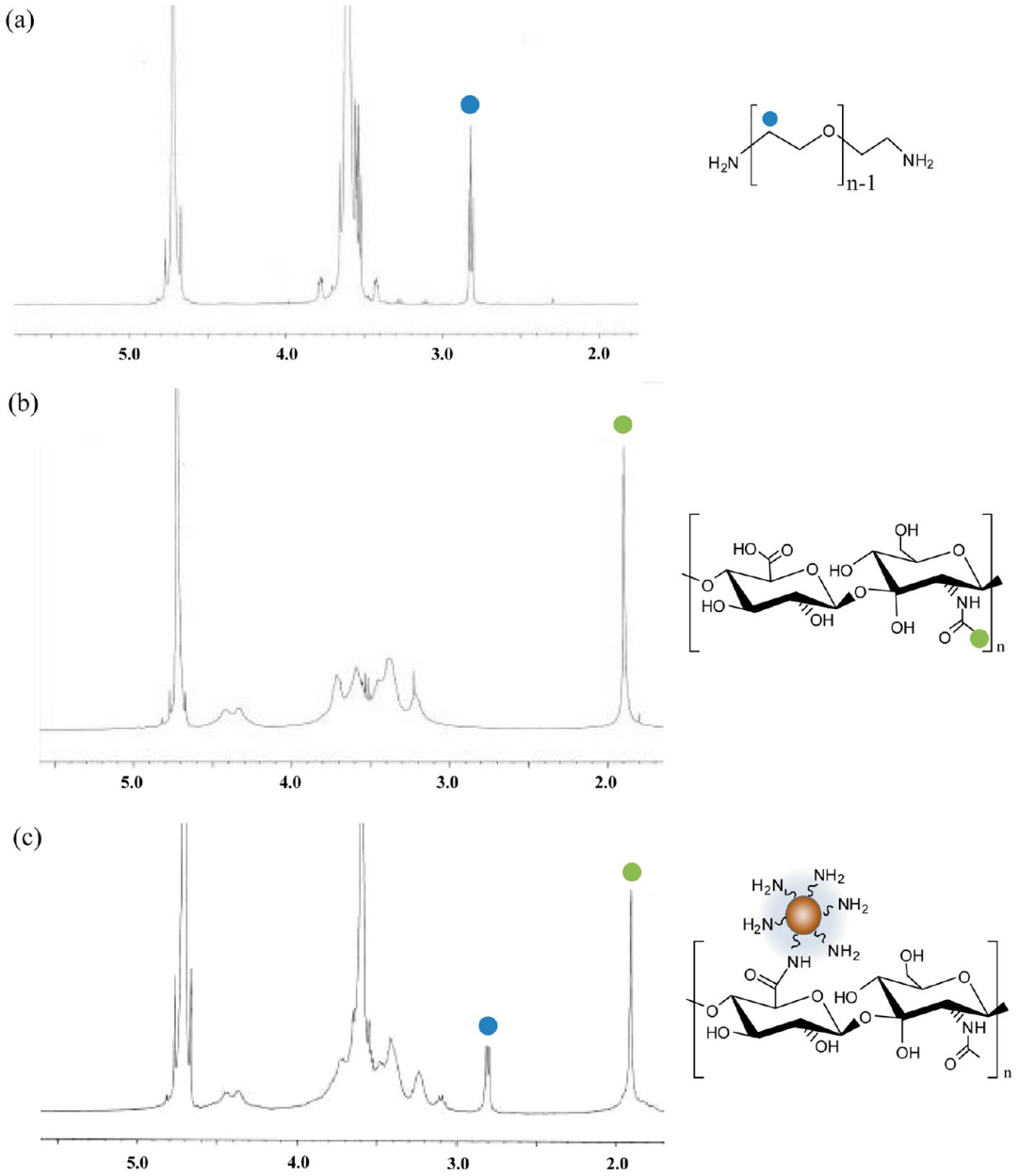

Figure 3. ^{1}H NMR spectra of (a) PEG diamine, (b) HA, and (c) HA−Cdot conjugate in D_2O.

In Vitro Bioimaging of Cdots and HA−Cdot Conjugates. B16F1 and HEK293 cells were seeded on an eight-chamber glass slide at a density of 2×10^4 cells/well and cultured in DMEM supplemented with 10 vol% of FBS and 1 wt % of antibiotics in a humidified 5% CO_2 incubator at 37 °C for 24 h. The culture medium was replaced with FBS-free DMEM. Then, 0.1 mg/mL of Cdots and 0.2 mg/mL of HA−Cdot conjugates in 300 μL of DMEM, which had the same PL intensity values, were added to the wells of culture slides. For HA preincubation tests, 100-fold molar excess of HA was added to the wells for 2 h before the treatment with HA−Cdot conjugates. The cells were incubated for 2 h, washed with PBS, fixed with 4 wt % paraformaldehyde in PBS, washed again with PBS twice, and observed with a confocal laser scanning microscope (FV1000, Olympus America Inc.) at a magnification of ×400. The internalized Cdots and HA−Cdot conjugates in the cytoplasm were excited with an Ar-green laser at 543 nm and an Ar-blue laser at 488 nm, respectively. An LD405 laser at 405 nm was used to visualize the DAPI.

In Vivo Bioimaging of Cdots and HA−Cdot Conjugates. Balb/c mice at an average age of 5 weeks were housed under a standard condition of a 12 h light/dark cycle with free access to food and water throughout the study period. The mice were anesthetized via intraperitoneal injection of a combination of ketamine (100 mg/kg) and xylazine (10 mg/kg). Cdot solution (50 μL, 0.1 mg/mL) and HA−Cdot conjugate solution (50 μL, 0.2 mg/mL) were subcutaneously injected on the back of Balb/c mice (n = 3). After injection, the mice were bioimaged using a luminescent image analyzer (IVIS Lumina, Xenogen, CA) with GFP excitation and emission filters. In addition, Cdot solution (50 μL, 0.1 mg/mL) and HA−Cdot solution (50 μL, 0.2 mg/mL) were intravenously injected into mice to investigate their body distribution (n = 3). PBS was used as a control. After 4 h, the organs were harvested for ex vivo bioimaging analysis. The fluorescence of injected Cdots and HA−Cdot conjugate was captured using the luminescent image analyzer with dsRed excitation and emission filters. We complied with the POSTECH institutional ethical use protocols for animals.

Statistical Analysis. The data are expressed as means ± standard deviation from several separate experiments. Statistical analysis was carried out via the two-way analysis of variance (ANOVA) test using the software of SigmaPlot12.0, and a value for $P < 0.05$ was considered statistically significant.

dx.doi.org/10.1021/bm300796q | *Biomacromolecules* 2012, 13, 2554−2561

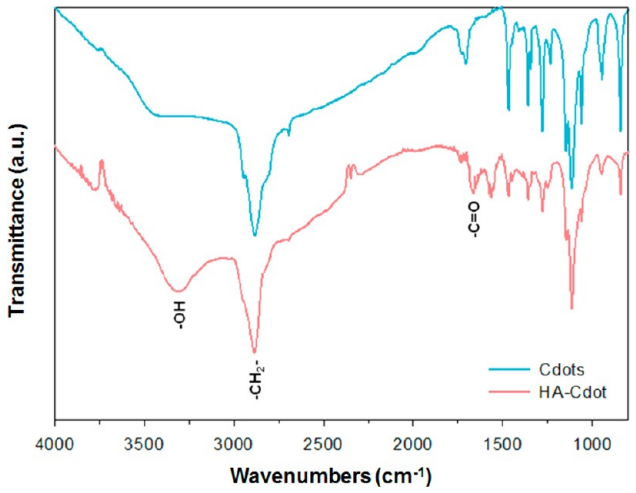

Figure 4. FT-IR spectra of Cdots and HA−Cdot conjugates.

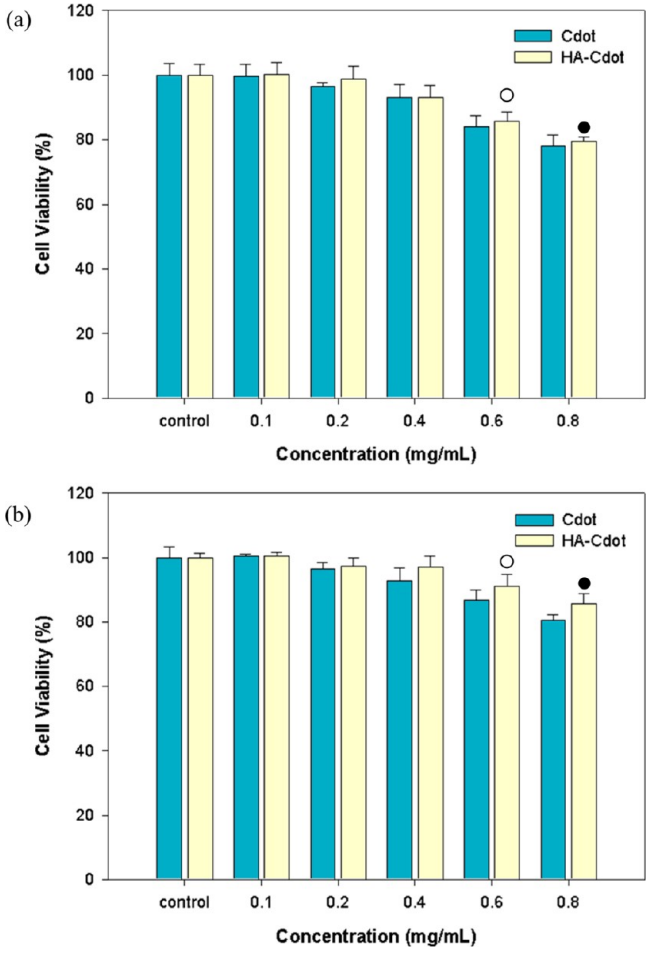

Figure 5. Cytotoxicity of Cdots and HA−Cdot conjugates with increasing concentrations from 0 to 0.8 mg/mL in (a) B16F1 cells and (b) HEK293 cells (○● $P < 0.05$ for the comparison between B16F1 and HEK293 cells).

RESULTS AND DISCUSSION

Preparation and Characterization of Cdots and HA−Cdot Conjugates. Scheme 1 shows the schematic illustration for the synthesis of Cdots and HA−Cdot conjugates using citric acid as a carbon precursor. Cdots were synthesized by the pyrolysis in the presence of PEG diamine as a capping material.

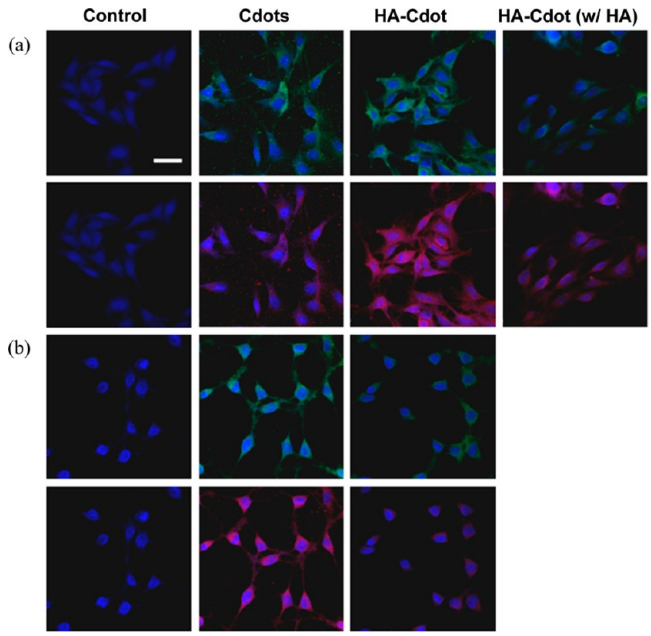

Figure 6. Confocal laser scanning microscopic images of (a) B16F1 and (b) HEK293 cells after incubation at 37 °C for 24 h with Cdots and HA−Cdot conjugates in the absence and presence of 100-fold molar excess HA. Scale bar indicates 30 μm.

HA−Cdot conjugates were synthesized by amide bond formation between carboxyl groups of HA and amine groups of Cdot−PEG-amine using the EDC chemistry. Figure 1a shows fluorescence images of Cdots and HA−Cdot conjugates under UV light. Cdots exhibited a strong fluorescence under UV excitation and different fluorescence colors depending on the excitation wavelengths. Figure 1b shows the absorption and emission spectra of Cdots (solid line) and HA−Cdot conjugates (dashed line). The peak emission band shifted to a long wavelength with increasing excitation wavelength. These unique optical characteristics could be explained by the size distribution of Cdots or emission trap distribution on Cdot surfaces as reported elsewhere.[29] The PL intensity of Cdots was maintained even after conjugation to HA. Figure 2a,b shows the representative AFM and HRTEM images of Cdots. Cdots had an almost spherical morphology with a diameter in the range of 5−7 nm. According to HRTEM analysis, the lattice spacing of Cdot was measured to be 0.25 nm from the observation that the summation of 10 peaks was approximately 2.5 nm. Cdots were quite close to the (100) facet of graphite. The results confirmed the successful synthesis of PEG diamine-capped Cdots. As shown in Figure 2c, HA−Cdot conjugates had a mean particle size of 68.00 ± 2.66 nm. Cdots with a dimension of ca. 6 nm might be randomly attached to the backbone of HA (MW = 100 kDa) with a chain length of ca. 250 nm.[35] Figure 3 shows ^{1}H NMR spectra of PEG diamine, HA, and HA−Cdot conjugate in D_2O. Among many peaks on ^{1}H NMR spectra, we focused on a peak at δ = 2.8 ppm for the methylene group of PEG diamine (Figure 3a) and a peak at δ = 1.9 ppm for the methyl group of HA (Figure 3b). As shown in Figure 3c, we could detect both the methylene peak of PEG diamine and the methyl peak of HA on the ^{1}H NMR spectrum of HA−Cdot conjugates. Cdots and HA−Cdot conjugates were also analyzed by FT-IR to confirm the conjugate formation (Figure 4). The spectrum of Cdots was identical to that reported elsewhere.[36] After conjugation of Cdots to HA, the broad peak around

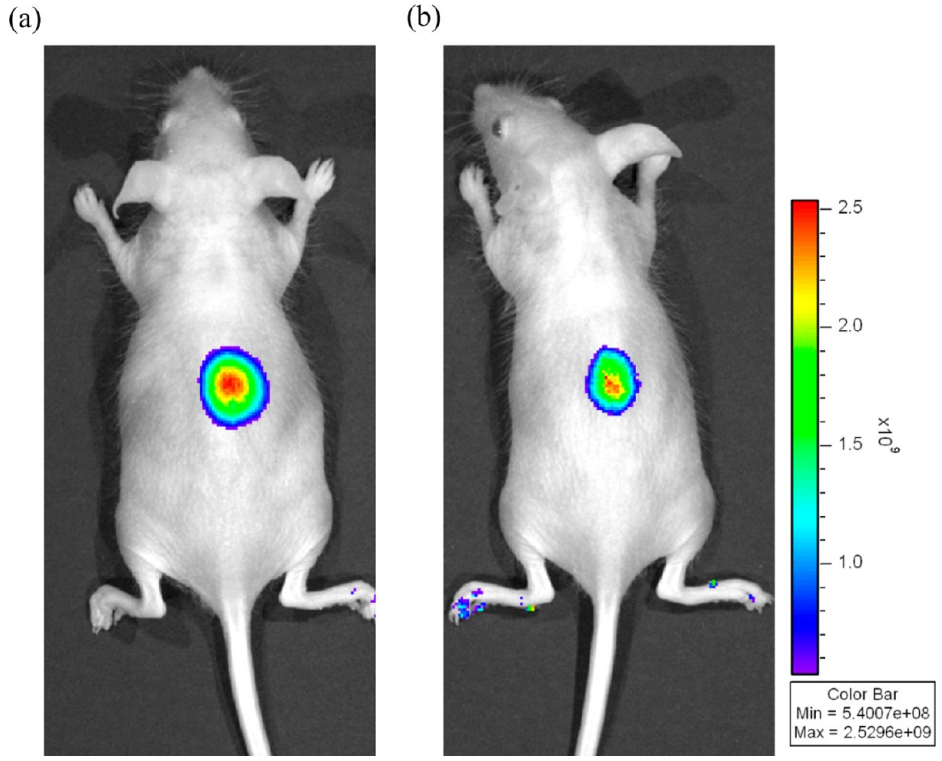

Figure 7. Fluorescence images of (a) Cdots and (b) HA−Cdot conjugates after subcutaneous injection to Balb/c mice.

3313 cm^{-1} on the FT-IR spectrum of HA−Cdot conjugates appeared corresponding to free hydroxyl groups of HA in the conjugates. The results from ^1H NMR and FT-IR analyses corroborated the successful formation of HA−Cdot conjugates.

Cytotoxicity of Cdots and HA−Cdot Conjugates. The cytotoxicity of Cdots and HA−Cdot conjugates was assessed by MTS assay in murine melanoma of B16F1 cells with HA receptors and human embryonic kidney cells of HEK293 cells without HA receptors, respectively. Figure 5 shows the cell viability after incubation with Cdots and HA−Cdot conjugates at a concentration of 0.1−0.8 mg/mL for 24 h. The results suggested that the cytotoxicity of Cdots and HA−Cdot conjugates was negligible up to a concentration of 0.4 mg/mL. Then, the cell viability gradually decreased with increasing concentration of Cdots. Meanwhile, B16F1 cells with HA receptors showed a lower cell viability than HEK293 cells possibly due to the enhanced cellular uptake of HA−Cdot conjugates by HA receptor mediated endocytosis. Statistical analysis revealed that the viability of HEK293 cells was significantly higher than that of B16F1 cells at the concentrations of 0.6 and 0.8 mg/mL ($P < 0.05$). In addition, the cytotoxicity of HA−Cdot conjugates appeared less than that of Cdots in HEK293 cells without HA receptors, which might be attributed to the reduced cellular uptake by the steric hindrance after conjugation of Cdots to HA. Overall, the cytotoxicity of Cdots was thought to be marginal considering the concentration of Cdots (0.1 mg/mL) for bioimaging applications.

In Vitro Bioimaging of Cdots and HA−Cdot Conjugates. Figure 6 shows confocal microscopic images of B16F1 and HEK293 cells after incubation with Cdots and HA-Cdot conjugates. We could observe strong green and red fluorescence from Cdot-labeled cells depending on the excitation wavelength, whereas no fluorescence was observed from the control sample without treatment. The positively charged Cdots with amine groups were effectively uptaken to the cells. By contrast, Cdots conjugated to negatively charged HA were thought to be uptaken by the HA receptor-mediated endocytosis. To confirm the HA receptor mediated endocytosis, we assessed the competitive cellular uptake of HA−Cdot conjugates in the presence of free HA. B16F1 cells were known to have HA receptors such as CD44 and LYVE-1.[31−33] As shown in Figure 6a, the cellular uptake of HA−Cdot conjugates was drastically reduced due to the competitive binding of HA to the receptors. By contrast, the cellular uptake of Cdots after conjugation to HA was significantly reduced in HEK293 cells without HA receptors (Figure 6b). The in vitro bioimaging results were well matched with those of MTS cytotoxicity tests. In other words, the enhanced cellular uptake by the HA receptor mediated endocytosis might be the reason for the slightly higher cytotoxicity of HA−Cdot conjugates in B16F1 cells than HEK293 cells (Figure 5). The in vitro bioimaging using Cdots confirmed the target specific intracellular delivery of HA derivatives to B16F1 cells with HA receptors.

In Vivo Bioimaging of Cdots and HA−Cdot Conjugates. On the basis of in vitro bioimaging study, we carried out in vivo real-time bioimaging of Cdots and HA−Cdot conjugates in Balb/c mice. Figure 7 shows the fluorescence images of Cdots and HA−Cdot conjugates after subcutaneous injection on the back of the mice. In both cases, we could observe the fluorescence of Cdots through the skin. Confirming the feasibility of Cdots for bioimaging applications, we further carried out bioimaging after intravenous injections of Cdots and HA−Cdot conjugates to investigate the whole-body distribution of HA derivatives. After 4 h postinjection, liver, kidney, and spleen were harvested for the fluorescence analysis ex vivo (Figure 8a). The fluorescence intensity of the dissected organs was quantified by the region-of-interest (ROI) method. Although the fluorescence intensity was not as strong, we could

dx.doi.org/10.1021/bm300796q | *Biomacromolecules* 2012, 13, 2554−2561

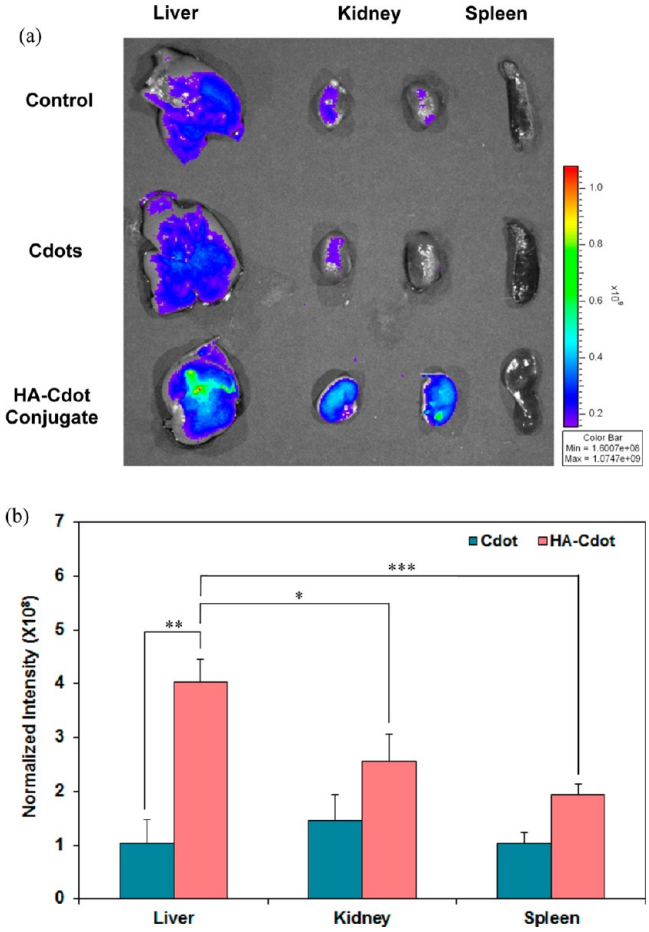

Figure 8. (a) Fluorescence images of dissected livers, kidneys, and spleens 4 h after tail-vein injections of Cdots or HA−Cdot conjugates. (b) Quantitative fluorescence analysis of Cdots and HA−Cdot conjugates in the dissected organs (*P < 0.05, **P < 0.005, ***P < 0.001).

confirm the target-specific delivery of HA−Cdot conjugates to the liver with abundant HA receptors such as HARE and CD44 by the receptor-mediated endocytosis (Figure 8b). The relatively low fluorescence intensity for the case of Cdots might reflect the rapid renal clearance of Cdots with a particle size in the range of 5−7 nm 4 h postinjection. The results were well matched with our previous reports on the real-time bioimaging of HA derivatives using Qdots.[34,35] Taken together, we could confirm the feasibility of HA derivatives as target-specific drug delivery carriers for the treatment of liver diseases and Cdots for various bioimaging applications. HA−Cdot conjugates will be investigated further for applications to theranostic systems, so-called diagnostic therapy.

CONCLUSIONS

Cdots were synthesized by the pyrolysis of citric acid in the presence of PEG diamine. PL spectroscopy, AFM, HRTEM, and FT-IR confirmed the successful synthesis of Cdots with a particle size of 5−7 nm. HA−Cdot conjugate was synthesized by amide bond formation between amine groups of Cdot and carboxylic groups of HA, which was corroborated by ^{1}H NMR and FT-IR analyses. The cytocompatibility of Cdots and HA−Cdot conjugates was confirmed by MTS assay. According to in vitro bioimaging, HA−Cdot conjugate was target-specifically delivered to B16F1 cells with HA receptors showing different fluorescence colors depending on the excitation wavelength. In addition, in vivo real-time bioimaging of Cdots and HA−Cdot conjugates revealed the target-specific delivery of HA−Cdot conjugates to the liver with HA receptors such as HARE and CD44, reflecting the feasibility of HA derivatives as a drug delivery carrier for the treatment of liver diseases and Cdots as a promising bioimaging agent.

AUTHOR INFORMATION

Corresponding Author

*Tel.: +82-54-279-2159; Fax: +82-54-279-2399. E-mail address: skhanb@postech.ac.kr.

Author Contributions

‖These authors contributed equally.

Notes

The authors declare no competing financial interest.

ACKNOWLEDGMENTS

This research was financially supported by the LG Yeonam Foundation Scholarship. This work was also financially supported by the Convergence Research Center Program through the National Research Foundation (NRF) of Korea funded by the Ministry of Education, Science and Technology (2009-0081871).

REFERENCES

(1) Eck, W.; Nicholson, A.; Zentgrat, H.; Semmler, W.; Bartling, S. *Nano Lett.* **2010**, *10*, 2318−2322.
(2) Liu, D.; Wu, W.; Ling, J.; Gu, N.; Zhang, X. *Adv. Func. Mater.* **2011**, *21*, 1498−1504.
(3) Michalet, X.; Pinaud, F. F.; Bentolila, L. A.; Tsay, J. M.; Doose, S.; Li, J. J.; Sundaresan, G.; Wu, A. M.; Gambhir, S. S.; Weiss, S. *Science* **2005**, *307*, 538−544.
(4) Gao, X.; Cui, Y.; Levenson, R. M.; Chung, W. L. K.; Nie, S. *Nat. Biotechnol.* **2004**, *22*, 969−976.
(5) Sharma, P.; Brown, S.; Walter, G.; Santra, S.; Moudgil, B. *Adv. Colloid Interface Sci.* **2006**, *123−126*, 471−485.
(6) Kim, S.; Lim, Y. T.; Soltesz, E. G.; Grand, A. D.; Lee, J.; Nakayama, A.; Parker, J. A.; Mihaljevic, T.; Laurence, R. G.; Dor, D. M.; Cohn, L. H.; Bawendi, M. G.; Fragioni, J. V. *Nat. Biotechnol.* **2003**, *22*, 93−97.
(7) So, M. K.; Xu, C.; Loening, A. M.; Gambhir, S. S.; Rao, J. *Nat. Biotechnol.* **2006**, *24*, 339−343.
(8) Medintz, I. L.; Uyeda, H. T.; Goldman, E. R.; Mattoussi, H. *Nat. Mater.* **2005**, *4*, 435−446.
(9) Derfus, A. M.; Chan, W. C. W.; Bhatia, S. N. *Nano Lett.* **2004**, *4*, 11−18.
(10) Dubertret, B.; Skourides, P.; Norris, D. J.; Noireaux, V.; Brivanlou, A. H.; Libchaber, A. *Science* **2003**, *298*, 1759−1762.
(11) Ballou, B.; Lagerholm, B. C.; Ernst, L. A.; Bruchez, M. P.; Waggoner, A. S. *Bioconjugate Chem.* **2004**, *15*, 79−86.
(12) Gerion, D.; Pinaud, F.; Williams, S. C.; Parak, W. J.; Zanchet, D.; Weiss, S.; Alivisatos, A. P. *J. Phys. Chem. B* **2011**, *105*, 8861−8871.
(13) Choi, H. S.; Liu, W.; Misra, P.; Tanaka, E.; Zimmer, J. P.; Ipe, B. I.; Bawendi, M. G.; Frangioni, J. V. *Nat. Biotechnol.* **2007**, *25*, 1165−1170.
(14) Manzoor, K.; Johny, S.; Thomas, D.; Setua, S.; Menon, D.; Nair, S. *Nanotechnology* **2009**, *20*, 65102.
(15) Li, H.; Shih, W. Y.; Shih, W. H. *Nanotechnology* **2007**, *18*, 205604.
(16) Liu, Z.; Robinson, J. T.; Sun, X.; Dai, H. *J. Am. Chem. Soc.* **2008**, *130*, 10876−10877.
(17) Luo, Z.; Vora, P. M.; Mele, E. J.; Johnson, A. T. C.; Kikkawa, J. M. *Appl. Phys. Lett.* **2009**, *94*, 111909.
(18) Eda, G.; Lin, Y. Y.; Mattevi, C.; Yamaguchi, H.; Chen, H. A.; Chen, I.; Chen, C.-W.; Chhowalla, M. *Adv. Mater.* **2009**, *22*, 505−509.

(19) Lee, A. J.; Wang, X.; Carlson, L. J.; Smyder, J. A.; Loesch, B.; Tu Zheng, X. M.; Krauss, T. D. *Nano Lett.* **2011**, *11*, 1636−1640.
(20) Loh, K. P.; Bao, Q.; Eda, G.; Chhowalla, M. *Nat. Chem.* **2010**, *2*, 1015−24.
(21) Hartschuh, A.; Pedrosa, H. N.; Novotny, L.; Krauss, T. D. *Science* **2003**, *301*, 1354−1356.
(22) Cherukuri, P.; Bachilo, S. M.; Litovsky, S. H.; Weisman, R. B. *J. Am. Chem. Soc.* **2004**, *126*, 15638−15639.
(23) Cherukuri, P.; Gannon, C. J.; Leeuw, T. K.; Schmidt, H. K.; Smalley, R. E.; Curley, S. A.; Weisman, R. B. *Proc. Natl. Acad. Sci. U.S.A.* **2006**, *103*, 18882−18886.
(24) Yang, K.; Wan, J.; Zhang, S.; Zhang, Y.; Lee, S. T.; Liu, Z. *ACS Nano* **2011**, *5*, 516−522.
(25) Zhou, J.; Booker, C.; Li, R.; Zhou, X.; Sham, T.; Sun, X.; Ding, Z. *J. Am. Chem. Soc.* **2007**, *129*, 744−745.
(26) Sun, Y. P.; Zhou, B.; Lin, Y.; Wang, W.; Fernando, K. A. S.; Pathak, P.; Meziani, M. J.; Harruff, B. A.; Wang, X.; Wang, H.; Luo, P. G.; Yang, H.; Kose, M. E.; Chen, B.; Veca, L. M.; Xie, S. Y. *J. Am. Chem. Soc.* **2006**, *128*, 7756−7757.
(27) Liu, H.; Ye, T.; Mao, C. *Angew. Chem., Int. Ed.* **2007**, *119*, 6593−6595.
(28) Bourlinos, A. B.; Stassinopoulos, A.; Anglos, D.; Zboril, R.; Karakassides, M.; Giannelis, E. P. *Small* **2008**, *4*, 455−458.
(29) Zhu, H.; Wang, X.; Li, Y.; Wang, Z.; Yang, F.; Yang, X. *Chem. Commun.* **2009**, *34*, 5118−5120.
(30) Baker, S. N.; Baker, G. A. *Angew. Chem., Int. Ed.* **2010**, *49*, 2−21.
(31) Wang, F.; Xie, Z.; Zhang, H.; Liu, C.; Zhang, Y. *Adv. Funct. Mater.* **2011**, *21*, 1027−1031.
(32) Zhu, A.; Qu, Q.; Shao, X.; Kong, B.; Tian, Y. *Angew. Chem., Int. Ed.* **2012**, DOI: 10.1002/anie.201109089.
(33) Tao, H.; Yang, K.; Ma, Z.; Wan, J.; Zhang, Y.; Kang, Z.; Liu, Z. *Small* **2012**, *8*, 281−290.
(34) Kim, K. S.; Hur, W.; Park, S. J.; Hong, S. W.; Choi, J. E.; Goh, E. J.; Yoon, S. K.; Hahn, S. K. *ACS Nano* **2010**, *4*, 3005−3014.
(35) Oh, E. J.; Park, K. T.; Kim, K. S.; Kim, J. S.; Yang, J.; Kong, J. H.; Lee, M. Y.; Hoffman, A. S.; Hahn, S. K. *J. Controlled Release* **2010**, *141*, 2−12.
(36) Wang, F.; Pang, S.; Wang, L.; Li, Q.; Kreiter, M.; Liu, C. *Chem. Mater.* **2010**, *22*, 4528−4530.